Q-band EPR cryoprobe

Vidmantas Kalendra [a,b], Justinas Turčak [a], Gediminas Usevičius [a], Hugo Karas [c],
Miriam Hülsmann [d], Adelheid Godt [d], Gunnar Jeschke [c], Jūras Banys [a], John J.L. Morton [e,f],
Mantas Šimėnas [a,*]

[a] *Faculty of Physics, Vilnius University, Sauletekio 3, LT-10257 Vilnius, Lithuania*
[b] *Amplify My Probe Ltd., London NW1 1NJ, UK*
[c] *Department of Chemistry and Applied Biosciences, ETH Zurich, Vladimir-Prelog-Weg 1-5/10, 8093 Zurich, Switzerland*
[d] *Faculty of Chemistry and Center for Molecular Materials (CM₂), Bielefeld University, Universitätsstraße 25, 33615 Bielefeld, Germany*
[e] *London Centre for Nanotechnology, University College London, London WC1H 0AH, UK*
[f] *Department of Electronic & Electrical Engineering, University College London, London WC1E 7JE, UK*

ARTICLE INFO

ABSTRACT

Following the success of cryogenic EPR signal preamplification at X-band, we present a Q-band EPR cryoprobe compatible with a standard EPR resonator. The probehead is equipped with a cryogenic ultra low-noise microwave amplifier and its protection circuit that are placed close to the sample in the same cryostat. Our cryoprobe maintains the same sample access and tuning which is typical in Q-band EPR, as well as supports high-power pulsed experiments on typical samples. The performance of our setup is benchmarked against that of existing commercial and home-built Q-band spectrometers, using CW EPR and pulsed EPR/ENDOR experiments to reveal a significant sensitivity improvement which reduces the measurement time by a factor of about 40× at 6 K temperature at reduced power levels.

1. Introduction

Cryogenically cooled cryoprobes containing cryogenic low-noise amplifiers (LNAs) have become a standard tool in NMR spectroscopy providing a substantial boost in sensitivity [1–4]. The thermal noise in these probeheads is significantly suppressed by simultaneous cooling of the LNA and NMR coil, independently of the sample temperature. Despite this widespread success in NMR, a signal preamplification with cryogenic LNAs is not yet widely used in EPR spectroscopy. Several earlier EPR studies have demonstrated promising sensitivity improvements using cryogenic amplifiers at different microwave frequency bands [5–11]. However, these setups have limited compatibility with commercial resonators and spectrometers, typical samples or high-power pulsed EPR experiments.

Recently, we modified a commercial X-band EPR probehead by equipping it with a cryogenic LNA and its protection circuit placed close to the sample in the same cryostat, while simultaneously satisfying the typical requirements of the EPR community [12]. For pulsed EPR experiments, our X-band cryoprobe provided a significant improvement of the voltage signal-to-noise ratio (SNR) by a factor close to 10× below 10 K, which gradually decreased to about 2× at room temperature. Such a high sensitivity enhancement has already enabled important

EPR studies of some intricate spin systems that would otherwise be nearly impossible with standard setups [13–15].

In a subsequent paper [16], we placed the LNA and its protection circuit in a separate cryostat, which provided EPR sensitivity improvement independent of sample temperature, while also facilitating the introduction of cryogenic preamplification to (more bulky) ENDOR and Q-band probeheads. However, due to the room-temperature microwave paths joining the sample and LNA cryostats, the SNR improvement was only moderate and approached a factor of 4× at X-band, which is substantially lower compared to the performance of the first design at low temperature [12]. The sensitivity enhancement for the Q-band setup was even smaller reaching only a factor of 2× and thus diverting attention back to the single-cryostat approach, which is explored in this work.

Here, we report design and performance of such a Q-band EPR cryoprobe equipped with a cryogenic LNA and its protection circuit, which are connected to a commercial Q-band resonator placed in a standard cryostat. Our probehead maintains ordinary sample access and resonator coupling, and is fully compatible with the high-power pulsed EPR experiments. We demonstrate the performance of our setup by performing CW EPR and pulsed EPR/ENDOR experiments of ordinary

---

* Corresponding author.
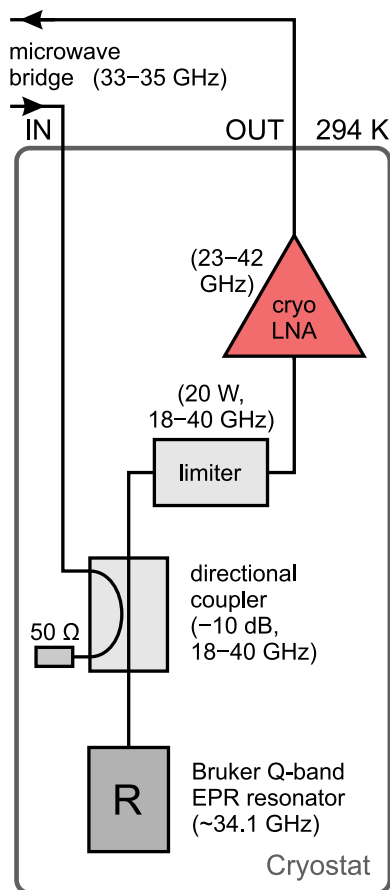 *E-mail address:* mantas.simenas@ff.vu.lt (M. Šimėnas).

Fig. 1. Schematic of the microwave circuit within our Q-band cryoprobe containing a cryogenic LNA. The probehead is connected to the microwave bridge using two microwave ports. In practice, all microwave components are closely packed close to the resonator.

samples. The probehead provides a significant voltage SNR improvement by a factor of about 6.5× at 6 K, which gradually approaches 1.5× at room temperature.

2. Probehead design

Our cryoprobe is based on a commercial Bruker EN5107D2 Q-band microwave resonator compatible with 1.6 mm outer diameter EPR tubes. It is designed to handle high power microwave pulses from a traveling-wave tube (TWT) amplifier, as well as to retain the conventional sample access and resonator coupling capabilities. Similarly to our previously reported X-band setup [12], the microwave circuit of our Q-band cryoprobe is based on a 10 dB directional coupler (Pasternack PE2CP1126-10), which is used to guide the microwave signals (Fig. 1). The incoming microwave pulses reach the resonator via the coupled port of the coupler, which also causes a partial suppression of the input thermal noise (see below) at the expense of pulse power [12,16]. The reflected microwave pulses and spin echoes coming from the resonator are guided by the same directional coupler to a Pasternack PE80L2002 (20 W peak power, 12 mW typical flat leakage, 63 mW maximum flat leakage, 10 ns recovery time, 0.1% duty cycle) limiter, which is used to protect a Low Noise Factory LNF-LNC23_42B cryogenic LNA (28 dB gain, 8 K noise temperature at 4 K and 34 GHz). The LNA is thermalized to the temperature of the sample via a C110 copper bracket extending below the resonator to the bottom of the cryostat. The amplified signal leaves the probehead via a second output microwave line connected to the EPR bridge.

Due to the limited space in the cryostat (Oxford CF935), we have chosen microwave components with the 2.92 mm type coaxial connectors instead of more bulky waveguides. The resonator, however, is connected to the directional coupler using a short WR-28 waveguide section with an attached waveguide-to-coax adapter. Employment of more lossy coaxial cables is acceptable, as the dominant cable length is either prior the directional coupler or after the LNA. A photograph of our probehead is given in Figure S1.

We also note that the cryoprobe has input and output ports that must be connected to the EPR bridge, while typical EPR spectrometers are designed to operate only in the reflection mode and thus have only one microwave port. As in our previous works [12,16], we solve this problem through a simple modification of the microwave bridge in which we bypass the internal circulator.

3. Experimental and calculation details

3.1. Pulsed EPR

Pulsed EPR experiments were performed using an IF-Q option of a Bruker ELEXSYS E580/IF-Q spectrometer equipped with a 10 W AmpQ-10 solid-state amplifier (SSA). For these experiments, we placed a small amount of the Bruker DEER test sample in a 1.6 mm outer diameter EPR tube. The SNR improvement was characterized using a Hahn echo pulse sequence ($\pi/2 - \tau - \pi - \tau -$ echo) with two-step phase cycling. Due to the 10 dB directional coupler, the pulse power reaching the sample was significantly reduced resulting in the shortest achievable π-pulse duration of about 200 ns in the overcoupled resonator.

A much shorter π-pulse of 40 ns was obtained on a homebuilt Q-band spectrometer equipped with a 150 W TWT amplifier. For these experiments, we measured a Cu(II) signal of a Cu(II)-nitroxide molecular ruler (Figure S2) sample (200 µM ruler concentration in 1:1 (v:v) mixture of D2O/d_8-glycerol) [17] placed in a 1.6 mm outer diameter EPR tube.

To avoid saturation of the digitizers, the interpulse delay τ was adjusted to produce a sufficiently weak echo signal. Depending on the sample temperature, the shot repetition time was chosen to be sufficiently long to allow full recovery of the signal.

The SNR and its uncertainty were determined using 10 separate measurements of the Hahn echo. The traces were corrected by subtracting constant backgrounds, which proved to be almost negligible. The intensity of the spin signal was taken as a maximum of the echo obtained by fitting a Gaussian peak function, while noise was calculated as the standard deviation of the signal far away from the echo (at least 500 data points were used for noise calculation).

The SNR improvement provided by our cryoprobe was benchmarked against standard reflection setups obtained by reattaching the resonator to the ordinary Bruker Q-band probehead. The resonator coupling arm was tightly fixed to avoid potential variations during switching between both setups. All parameters, except for the microwave power and negligible changes in the microwave frequency and magnetic field, were kept constant in both measurements. The microwave power was adjusted to yield the same duration of the π-pulse, and the field position was verified by the echo-detected field sweep (EDFS) experiments obtained using the same Hahn echo pulse sequence.

3.2. Pulsed ENDOR

We performed pulsed ^{1}H ENDOR experiments at 10 K using the Bruker ELEXSYS E580/IF-Q spectrometer equipped with a Bruker DICE ENDOR system and a 150 W radiofrequency amplifier. The measurements were performed using the same Bruker DEER test sample placed in a 1.6 mm outer diameter EPR tube, which was inserted into the overcoupled EPR resonator. The Mims pulse sequence [18] was used with the microwave $\pi/2$-pulse length of 100 ns and the radiofrequency

π-pulse of 8 µs. The interpulse delay τ between the microwave pulses was set to 3 µs to yield a sufficiently weak echo signal. Analogous to the pulsed EPR case, the SNR improvement of ENDOR experiments was benchmarked against a standard setup measured in reflection. The power of the radiofrequency pulse was carefully adjusted to yield the same ENDOR efficiency in both cases. For SNR improvement calculation, the ENDOR spectra were baseline corrected and noise was determined by calculating the standard deviation of signal far away from the ENDOR lines.

3.3. CW EPR

We used a standard coal sample to benchmark the SNR improvement for the CW EPR experiments at 50 K. The measurements were performed using the same Bruker ELEXSYS E580/IF-Q spectrometer, critically coupled resonator, and 1 G and 50 kHz modulation of the external field. The SNR improvement was calculated by comparing the noise levels after the baseline correction and normalization of the spin line obtained using the cryoprobe and unmodified setups.

3.4. Calculation of sensitivity improvement

The SNR improvement was calculated using the approach developed in our previous work [16], which is based on the effective noise temperature formalism [7]. We define the sensitivity improvement provided by the cryoprobe as the output voltage SNR ratio between the cryoprobe (C) and unmodified (U) setups:

$$\frac{\text{SNR}_{\text{out}}^{\text{C}}}{\text{SNR}_{\text{out}}^{\text{U}}} = \sqrt{\frac{F^{\text{U}}}{F^{\text{C}}} \frac{T_{\text{in}}^{\text{U}}}{T_{\text{in}}^{\text{C}}}}. \tag{1}$$

Here, F and T_{in} denote the noise factor of the microwave circuit and the noise temperature at its input, respectively. The noise factor can be calculated from the total effective noise temperature T_{e} as

$$F = 1 + \frac{T_{\text{e}}}{T_{\text{in}}}, \tag{2}$$

where T_{e} can be obtained using the Friis equation [16,19].

In our calculations, we assume $T_{\text{in}}^{\text{U}} = 294$ K independent of the sample temperature, since in a standard setup the sample is not isolated from room temperature thermal noise. In contrast, as demonstrated in our previous works [12,16], additional attenuation on the cold input line of the EPR cryoprobe provides this isolation, and thus T_{in}^{C} may be significantly lower than 294 K. Our current setup is equipped with a 10 dB directional coupler, which provides 10× reduction in the input thermal noise power resulting in $T_{\text{in}}^{\text{C}} = 30$ K for sample temperature T_S lower than 30 K. For $T_S > 30$ K, we set $T_{\text{in}}^{\text{C}} = T_S$.

To calculate the noise factor of the cryoprobe and Bruker setups, we measured their microwave losses using a vector network analyzer (VNA). The measurement results are summarized in Figure S3. The gain and noise temperature of the LNAs were taken from the manufacturer specifications.

4. Results and discussion

First, we investigated the performance of our Q-band cryoprobe by measuring the Hahn echo of a Bruker DEER test sample at 10 K and comparing it to the unmodified Bruker setup. A comparison of the obtained echoes are presented in Fig. 2a showing that our cryoprobe provides a highly significant voltage SNR improvement by a factor of about 6×, which translates to the measurement time reduction close to 35× at 10 K. The obtained sensitivity gain at this temperature is about 3× higher compared to our previously reported external cryoprobe case [16]. A significantly better performance of our current setup mainly originates from the suppression of the input thermal noise by the 10 dB directional coupler and the absence of the room-temperature microwave paths prior the cryogenic LNA.
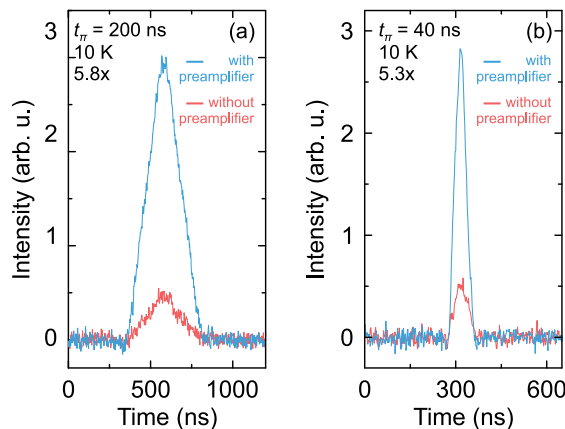

Fig. 2. Hahn echoes of the (a) Bruker DEER sample and (b) Cu(II)-nitroxide molecular ruler obtained at 10 K using (a) 10 W SSA and (b) 150 W TWT. The echoes are normalized to the noise level. Experimental parameters: (a) $\tau = 5.5$ µs, 1 average, $t_\pi = 200$ ns, and (b) $\tau = 12$ µs, 20 averages, $t_\pi = 40$ ns.

The suppression of the input thermal noise occurs at the expense of pulse power limiting the π-pulse duration to 200 ns with a 10 W SSA. To assess the compatibility of our probehead with high-power pulses, we switched to a homebuilt Q-band spectrometer equipped with a 150 W TWT amplifier. For this purpose, we measured a Hahn echo of a Cu(II) signal from a Cu(II)-nitroxide molecular ruler sample (see experimental details) at 10 K temperature. A comparison of the echoes obtained using our cryoprobe and unmodified setups is presented in Fig. 2b indicating a sensitivity improvement of 5.3×, which is slightly lower compared to the low-power measurement. This small discrepancy can be attributed to slightly lower losses (by about 0.5 dB) of the homebuilt spectrometer compared to the Bruker setup. The measurements with the TWT show a compatibility of our Q-band cryoprobe with high-bandwidth pulsed EPR experiments. A shorter π-pulse duration might be achieved by reducing the losses of the input microwave path, using a more powerful TWT amplifier or a lower coupling directional coupler (e.g. 6 dB), provided that the peak power (20 W) of the limiter is not exceeded.

We also measured the EDFS spectra of the Bruker DEER test sample (6 K) and Cu(II)-nitroxide molecular ruler (10 K) with the cryoprobe and unmodified setups (Fig. 3). The obtained spectra reveal similar SNR improvements as determined from the Hahn echo experiments. These experiments also demonstrate that the cryoprobe does not affect the lineshapes indicating no saturation effects for signals of moderate intensity.

We investigated the temperature dependence of the SNR improvement by performing the Hahn echo experiments starting at 6 K and warming up to room temperature, which revealed a gradual decrease of the sensitivity gain from 6.5× to about 1.5× (Fig. 4). A remaining small sensitivity improvement at room temperature indicates that our cryoprobe setup has lower microwave losses prior the LNA compared to the Bruker setup. A similar behavior was also observed in our previous designs of the X-band cryoprobe [12,16].

We used a VNA to determine the microwave losses of our cryoprobe and unmodified setups (see Figure S3) allowing us to compare the measured sensitivity improvement with our theoretical model given by Eq. (1). The calculated temperature dependence of the SNR improvement is also presented in Fig. 4 revealing a good agreement with the experimental results. A small discrepancy may originate from the unaccounted sources of uncertainty, which are difficult to quantify in practise (e.g. temperature gradients, changes of insertion loss with temperature).

Our model also allows to predict the sensitivity gain for highly attenuated input line, which in practise could be achieved using a
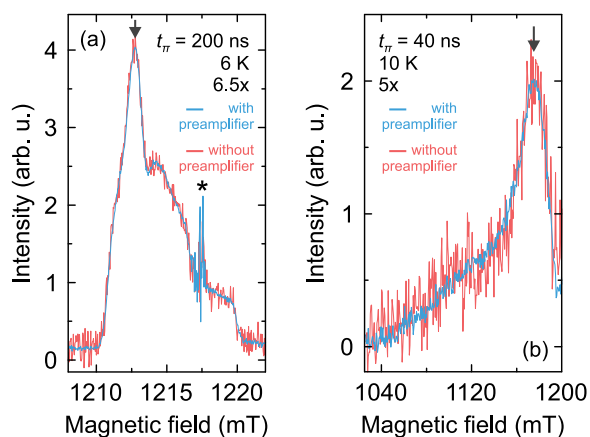
Fig. 3. EDFS of the (a) Bruker DEER sample and (b) Cu(II) signal of the Cu(II)-nitroxide molecular ruler obtained using (a) 10 W SSA and (b) 150 W TWT. The EDFSs are normalized to the signal level. Arrows mark field positions, at which other EPR experiments were performed. The asterisk in (a) indicates E' centers present in the clear fused quartz sample tube. Experimental parameters: (a) $\tau = 6$ μs, 1 average, $t_\pi = 200$ ns, 6 K, and (b) $\tau = 12$ μs, 4 averages, $t_\pi = 40$ ns, 10 K.
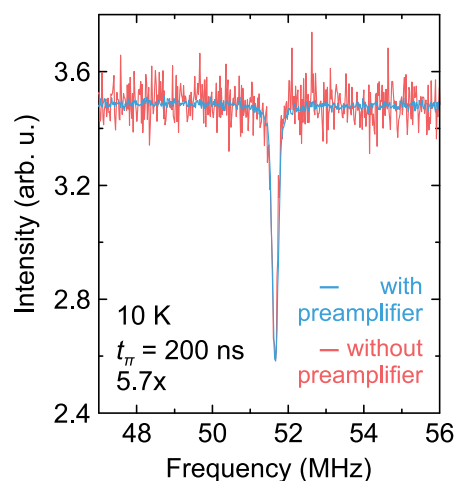

Fig. 5. ^{1}H Mims ENDOR spectrum of the Bruker DEER sample obtained at 10 K with and without the cryoprobe with the corresponding voltage SNR improvements of 5.7×. Experimental parameters: $\tau = 3$ μs, 1 average, $t_\pi = 200$ ns (10 W SSA), $t_{rf} = 8$ μs.
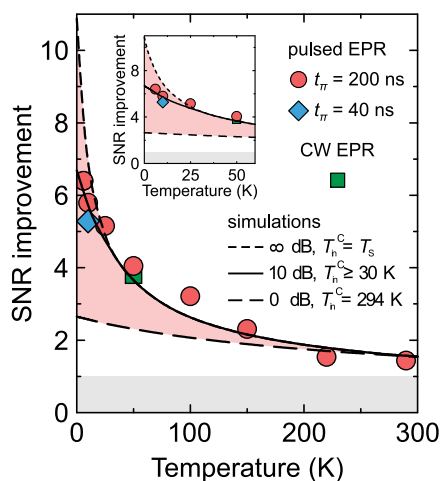
Fig. 4. SNR improvement vs. sample (cryoprobe) temperature measured using Hahn echo experiments with Bruker (10 W SSA, red circles) and homebuilt (150 W TWT, blue diamond) Q-band spectrometers. The green square shows the improvement obtained for the CW EPR experiment. The low-temperature region is presented in the inset. Solid curve shows the calculated SNR improvement (10 dB input attenuation, $T_{in}^C \geq 30$ K) based on the measured microwave losses of our cryoprobe and Bruker setups. Pink area indicates the region of theoretical SNR enhancement bounded by the dashed curves representing the cases of the full (∞ dB input attenuation, $T_{in}^C = T_S$) and no suppression (0 dB, $T_{in}^C = T_{in}^U = 294$ K) of the input thermal noise. The gray region marks SNR improvement less than one. The error bar is about the size of the data point.

20–30 dB directional coupler. In this case, $T_{in}^C = T_S$ in the whole range of accessible sample temperature T_S. For such a setup, the SNR enhancement would approach a factor of 10× at 4 K providing an impressive 100-fold reduction in the measurement time (Fig. 4). Such a high input attenuation may still be exploited for high-spin systems (e.g. Mn(II) or Gd(III)), which require significantly lower power for a π-pulse, although the provided sensitivity gain may not outweigh the reduced bandwidth effect. Note that above 30 K, the additional attenuation does not provide higher SNR improvement compared to the 10 dB case, as 10 dB input attenuation corresponds to $T_{in}^C \geq 30$ K.

We also calculated the lower bound of the sensitivity enhancement provided by our cryoprobe by assuming no input attenuation (Fig. 4) and thus no suppression of the input thermal noise ($T_{in}^C = 294$ K). In such a case, the SNR improvement still approaches a substantial factor

of about 2.6× below 10 K. Note that a practical implementation of such a setup is more challenging, as it requires a ferrite circulator to be placed in the magnetic field at low temperature in the vicinity of the sample instead of a directional coupler.

Our probehead design also allows us to perform ENDOR experiments. We benchmarked the ENDOR sensitivity gain at 10 K using the Mims ENDOR pulse sequence and Bruker DEER test sample. The ^{1}H ENDOR spectra obtained using the cryoprobe and unmodified setups are presented in Fig. 5 revealing the SNR improvement factor of 5.7×, which is in a good agreement with the Hahn echo experiments. This indicates a full compatibility of our Q-band cryoprobe with the pulsed ENDOR experiments.

We also tested the performance of our cryoprobe for the CW EPR experiments. Fig. 6 shows the CW EPR spectrum of a coal sample measured at 50 K using the cryoprobe and unmodified setups. The obtained SNR improvement is about 3.8× in a very good agreement with the pulsed EPR experiments (see Fig. 4) demonstrating that our probehead is also compatible with the CW EPR spectroscopy. Here, we note that, due to the additional 10 dB attenuation on the input path, the CW sensitivity improvement provided by the cryoprobe is only beneficial for spin systems, which are easy to saturate, which is fairly typical at low temperature.

Here, we also address the issue of the reduced excitation bandwidth for pulsed EPR experiments, which would limit the absolute sensitivity of our cryoprobe provided higher excitation bandwidth is not available. This effect would be especially pronounced for DEER experiments, where both pump and probe excitation bandwidths contribute multiplicatively to the DEER signal. To estimate this effect, we calculated the DEER signal for a typical nitroxide spin system by comparing 20 ns and 40 ns π-pulse durations (see Supplementary material for details). The former case is achievable with typical unmodified setups, while the later duration is our cryoprobe limit. Our calculations show that such a difference in bandwidth (40 ns vs. 20 ns) corresponds to a significant 2.8× decrease in the overall DEER sensitivity. By taking this into account, at 50 K, where typical nitroxide DEER experiments are performed, the cryoprobe would provide 1.5× SNR improvement instead of currently obtained 4× (see Fig. 4). Below 10 K, this factor would be about 2.2×. Thus, for situations, where the excitation bandwidth cannot be increased, the performance of our setup for DEER experiments would become comparable to the previously reported design of the external cryoprobe [16].

Note that using a 6 dB directional coupler instead of a 10 dB version would allow us to reduce the π-pulse duration to about 26 ns.
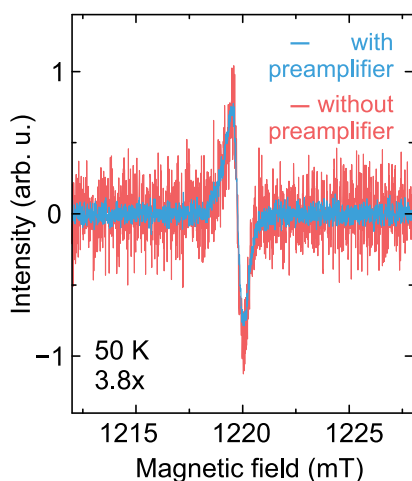
Fig. 6. Normalized CW EPR spectrum of the coal sample obtained at 50 K with and without the cryoprobe with the corresponding voltage SNR improvements of 3.8×. Experimental parameters: 0.01 μW, 1 average, modulation field: 1 G and 50 kHz.

Our simulations show that such a difference in pulse duration (40 ns vs. 26 ns) results in a factor of about 1.9× in the DEER sensitivity. However, the reduced coupling attenuation also provides a worse SNR improvement of our cryoprobe due to higher input thermal noise and a higher fraction of the spin signal lost to the input path. Our calculations based on the Friis equation show that the SNR improvement provided by the cryoprobe would be about 1.7× lower at 50 K when using a 6 dB coupler almost cancelling the benefit from the increased pulse bandwidth.

Lastly, we also note several practical aspects related to the cryoprobe usage and lifetime of the LNA. A typical flat leakage power of the limiter is 12 mW, which is significantly higher than the specified maximum CW power for safe operation of the LNA (0.1 mW). The peak power of the LNA relevant for pulsed EPR experiments is not specified by the manufacturer, but must be substantially higher, as during the extensive benchmarking of the cryoprobe, we have not observed any LNA aging effects. During testing, the cryoprobe also experienced drastic temperature changes (e.g. multiple insertions into a cold cryostat), which did not cause any issues with the performance.

5. Conclusions

In this work, we constructed and tested a Q-band EPR cryoprobe based on a commercial microwave resonator and a cryogenic ultra low-noise microwave preamplifier. Our cryoprobe is compatible with high power microwave pulses, while simultaneously maintaining the convenient sample access and resonator coupling capabilities, which allow CW EPR and pulsed EPR/ENDOR experiments with greatly enhanced sensitivity.

Measurements of the Hahn echo experiments demonstrated the SNR improvement by a factor of 6.5× at 6 K, which gradually decreased to about 1.5× at room temperature. Our calculations revealed that the sensitivity gain may be further improved by a higher suppression of the input thermal noise and reduction of the microwave losses prior the LNA. As discussed in our previous works, cooling of the LNA and the sample should be ultimately decoupled partially eliminating the observed decrease of the sensitivity gain with increasing sample temperature.

Our microwave circuit and probehead design should be also compatible with other Q-band microwave resonators such as broadband 3 mm tube resonators [20]. A full exploitation of wide bandwidth resonators for spin-1/2 species, however, would be impeded by the increased duration of the π-pulse due to the 10 dB directional coupler. This problem can be solved by using higher power TWT amplifiers and lower coupling directional couplers, provided the peak power of the limiter is not exceeded. Frequency-swept pulses may be also employed to extend the excitation bandwidth [21,22] provided that a substantially longer duration of such pulses is not the limiting factor.

In general, the obtained sensitivity gains may be used to reduce the spin concentration or sample volumes allowing advanced Q-band EPR experiments (e.g. dipolar spectroscopy [23–26]) with increased sensitivity.

CRediT authorship contribution statement

Vidmantas Kalendra: Conceptualization, Data curation, Funding acquisition, Investigation, Methodology, Project administration, Validation. **Justinas Turčak:** Formal analysis, Investigation, Software. **Gediminas Usevičius:** Investigation. **Hugo Karas:** Resources. **Miriam Hülsmann:** Resources. **Adelheid Godt:** Resources, Supervision. **Gunnar Jeschke:** Resources, Supervision. **Jūras Banys:** Funding acquisition, Project administration, Resources, Supervision. **John J.L. Morton:** Conceptualization, Resources, Supervision. **Mantas Šimėnas:** Conceptualization, Data curation, Formal analysis, Funding acquisition, Investigation, Methodology, Project administration, Resources, Software, Supervision, Validation, Visualization, Writing – original draft, Writing – review & editing.

Declaration of competing interest

The authors declare the following financial interests/personal relationships which may be considered as potential competing interests: Mantas Šimėnas reports a relationship with Amplify My Probe Ltd. that includes: equity or stocks. Vidmantas Kalendra reports a relationship with Amplify My Probe Ltd. that includes: equity or stocks

Data availability

Data needed to evaluate the conclusions in the paper can be found at http://dx.doi.org/10.18279/MIDAS.SPECTR.203438. Additional data related to this paper may be requested from the authors.

Data and materials availability

Data needed to evaluate the conclusions in the paper can be found at http://dx.doi.org/10.18279/MIDAS.SPECTR.203438. Additional data related to this paper may be requested from the authors.

Appendix A. Supplementary data

Supplementary material related to this article can be found online at https://doi.org/10.1016/j.jmr.2023.107573.

References

[1] P. Styles, N. Soffe, C. Scott, D. Crag, F. Row, D. White, P. White, A high-resolution NMR probe in which the coil and preamplifier are cooled with liquid helium, J. Magn. Reson. (1969) 60 (1984) 397–404.

[2] P. Styles, N.F. Soffe, C.A. Scott, An improved cryogenically cooled probe for high-resolution NMR, J. Magn. Reson. (1969) 84 (1989) 376–378.

[3] L. Darrasse, J.-C. Ginefri, Perspectives with cryogenic RF probes in biomedical MRI, Biochimie 85 (2003) 915–937.

[4] H. Kovacs, D. Moskau, M. Spraul, Cryogenically cooled probes - a leap in NMR technology, Prog. Nucl. Magn. Reson. Spectrosc. 46 (2005) 131–155.

[5] W.J. Wallace, R.H. Silsbee, Microstrip resonators for electron-spin resonance, Rev. Sci. Instrum. 62 (1991) 1754–1766.

[6] H.E. Altink, T. Gregorkiewicz, C.A.J. Ammerlaan, Sensitive electron paramagnetic resonance spectrometer for studying defects in semiconductors, Rev. Sci. Instrum. 63 (1992) 5742–5749.

[7] S. Pfenninger, W. Froncisz, J. Hyde, Noise analysis of EPR spectrometers with cryogenic microwave preamplifiers, J. Magn. Reson. Ser. A 113 (1995) 32–39.

[8] G.A. Rinard, R.W. Quine, R. Song, G.R. Eaton, S.S. Eaton, Absolute EPR spin echo and noise intensities, J. Magn. Reson. 140 (1999) 69–83.

[9] S. Vasilyev, J. Järvinen, E. Tjukanoff, A. Kharitonov, S. Jaakkola, Cryogenic 2 mm wave electron spin resonance spectrometer with application to atomic hydrogen gas below 100 mK, Rev. Sci. Instrum. 75 (2004) 94–98.

[10] R. Narkowicz, H. Ogata, E. Reijerse, D. Suter, A cryogenic receiver for EPR, J. Magn. Reson. 237 (2013) 79–84.

[11] Y. Artzi, Y. Twig, A. Blank, Induction-detection electron spin resonance with spin sensitivity of a few tens of spins, Appl. Phys. Lett. 106 (2015) 084104.

[12] M. Šimėnas, J. O'Sullivan, C.W. Zollitsch, O. Kennedy, M. Seif-Eddine, I. Ritsch, M. Hülsmann, M. Qi, A. Godt, M.M. Roessler, G. Jeschke, J.J. Morton, A sensitivity leap for X-band EPR using a probehead with a cryogenic preamplifier, J. Magn. Reson. 322 (2021) 106876.

[13] K.H. Richardson, J.J. Wright, M. Šimėnas, J. Thiemann, A.M. Esteves, G. McGuire, W.K. Myers, J.J.L. Morton, M. Hippler, M.M. Nowaczyk, G.T. Hanke, M.M. Roessler, Functional basis of electron transport within photosynthetic complex I, Nature Commun. 12 (2021) 5387.

[14] J. O'Sullivan, O.W. Kennedy, C.W. Zollitsch, M. Šimėnas, C.N. Thomas, L.V. Abdurakhimov, S. Withington, J.J. Morton, Spin-resonance linewidths of bismuth donors in silicon coupled to planar microresonators, Phys. Rev. Appl. 14 (2020) 064050.

[15] M. Šimėnas, J. O'Sullivan, O.W. Kennedy, S. Lin, S. Fearn, C.W. Zollitsch, G. Dold, T. Schmitt, P. Schüffelgen, R.-B. Liu, J.J.L. Morton, Near-surface ^{125}Te$^+$ spins with millisecond coherence lifetime, Phys. Rev. Lett. 129 (2022) 117701.

[16] V. Kalendra, J. Turčak, J. Banys, J.J. Morton, M. Šimėnas, X- and Q-band EPR with cryogenic amplifiers independent of sample temperature, J. Magn. Reson. 346 (2023) 107356.

[17] K. Keller, I. Ritsch, H. Hintz, M. Hülsmann, M. Qi, F.D. Breitgoff, D. Klose, Y. Polyhach, M. Yulikov, A. Godt, G. Jeschke, Accessing distributions of exchange and dipolar couplings in stiff molecular rulers with cu(ii) centres, Phys. Chem. Chem. Phys. 22 (2020) 21707–21730.

[18] W.B. Mims, Pulsed endor experiments, Proc. R. Soc. Lond. Ser. A Math. Phys. Eng. Sci. 283 (1965) 452–457.

[19] H. Friis, Noise figures of radio receivers, Proc. IRE 32 (1944) 419–422.

[20] Y. Polyhach, E. Bordignon, R. Tschaggelar, S. Gandra, A. Godt, G. Jeschke, High sensitivity and versatility of the DEER experiment on nitroxide radical pairs at Q-band frequencies, Phys. Chem. Chem. Phys. 14 (2012) 10762–10773.

[21] A. Doll, G. Jeschke, Wideband frequency-swept excitation in pulsed EPR spectroscopy, J. Magn. Reson. 280 (2017) 46–62.

[22] B. Endeward, M. Bretschneider, P. Trenkler, T.F. Prisner, Implementation and applications of shaped pulses in EPR, Prog. Nucl. Magn. Reson. Spectrosc. 136–137 (2023) 61–82.

[23] M. Pannier, S. Veit, A. Godt, G. Jeschke, H. Spiess, Dead-time free measurement of dipole-dipole interactions between electron spins, J. Magn. Reson. 142 (2000) 331–340.

[24] G. Jeschke, M. Pannier, A. Godt, H. Spiess, Dipolar spectroscopy and spin alignment in electron paramagnetic resonance, Chem. Phys. Lett. 331 (2000) 243–252.

[25] P.P. Borbat, J.H. Freed, Multiple-quantum ESR and distance measurements, Chem. Phys. Lett. 313 (1999) 145–154.

[26] S. Milikisyants, F. Scarpelli, M.G. Finiguerra, M. Ubbink, M. Huber, A pulsed EPR method to determine distances between paramagnetic centers with strong spectral anisotropy and radicals: The dead-time free RIDME sequence, J. Magn. Reson. 201 (2009) 48–56.